

## Original Article

# Experimental study on effects of a new type of interventional embolization agent in chemoembolization of liver transplantation tumors

Kaiyuan Xu<sup>1</sup>, Dandan Xiao<sup>2</sup>

Departments of <sup>1</sup>Radiology, <sup>2</sup>Outpatient, Shenzhen Hospital, Southern Medical University, Shenzhen 518010, China

Received February 21, 2019; Accepted May 10, 2019; Epub July 15, 2019; Published July 30, 2019

**Abstract:** The aims of this study were to observe the effects of doxorubicin (ADM)-alginate microspheres on rabbit VX2 liver transplantation tumor by transcatheter arterial chemoembolization (TACE). A total of 30 New Zealand white rabbits were transplanted 1-mm<sup>3</sup> mass of VX2 liver transplantation tumor and then were randomly divided into five groups: the normal saline group (group A), the blank microsphere group (group B), the ADM microsphere group (group C), the super-liquefied lipiodol group (UFLP, group D), and the UFLP + ADM group (group E) for comprising the conditions of apoptosis by TdT-mediated dUTP Nick-End Labeling (TUNEL) and growth rate/necrotic rate of orthotopic transplantation tumors in different groups by immunohistochemical staining of vascular endothelial growth factor (VEGF) and CD31 antibodies. The tumor volume in each group increased, but the growth was inhibited than group A. The number of intrahepatic and distant metastasis decreased in group C ( $P < 0.05$ ), and expression of VEGF and microvessel density (MVD) decreased ( $P < 0.01$ ). The number of cells undergoing apoptosis increased ( $P < 0.01$ ), and the apoptotic indexes in the five groups were 0.3%, 11.4%, 14.3%, 1.7%, and 5.1%, respectively ( $P < 0.01$ ). ADM microspheres can inhibit tumor volume growth and distant metastasis in TACE.

**Keywords:** Alginate-microsphere, VEGF, embolization, neoplastic transplantation, liver neoplasm

## Introduction

Primary liver and biliary cancers are very aggressive tumors [1]. Approximately 80% of patients diagnosed with hepatocellular carcinoma at an early stage are not candidates for surgical resection or transplantation [2], surgical treatment is the main option for cure or long term survival, and if the future liver remnant (FLR) is too small to meet the needs of liver function and volume, these patients are considered as unresectable [3], and then thermal ablation, such as radiofrequency ablation [4], microwave ablation [5] or high-intensity focused ultrasound (HIFU) ablation [6], are always alternative treatment choices for these people. Portal vein embolization (PVE) is a common strategy currently used to increase the FLR before major liver resection [7].

This study used the rabbit VX2 transplant tumor post-embolization metastasis model to simulate primary liver tumor in the clinic [8, 9], which

is a regular model of primary hepatocellular carcinoma [10].

It has been proven that many antitumor drugs are more effective than lipiodol [11, 12], we also chose ADM as the positive drug in our study, and the evaluation method to compare the efficiency of VX2 liver tumor after TACE has been mentioned in many literatures, such as microvessel density (MVD), which can assess tumor angiogenesis of VX2 liver tumor model noninvasively, and ethanol which has no significant impact on angiogenesis of viable tumor 1 week later after percutaneous ethanol injection [13].

In this study, the anti-tumor angiogenesis and mechanism of ADM-alginate microspheres were studied *in vivo* by interventional radiology, and the value of sodium alginate microspheres in inhibiting the recurrence and metastasis of liver cancer after chemotherapy and embolization was investigated. The data provide more

experimental basis for further clinic application of new embolic agents.

### Materials and methods

#### Animals

A total of 30 New Zealand white rabbits, weighing 2.5 to 3 kg, received open surgery to expose the liver. One pair of ophthalmological scissors was used to cut a small opening of about 3-5 mm in the left or right central lobe of the liver with about 5 mm in depth. The prepared VX2 tumor block of about 1 mm<sup>3</sup> was then directly implanted into the liver. Two weeks later, enhanced CT examination was performed to observe the size and growth of the tumor mass in the liver, as well as the maximum diameter (dmax) and the minimum diameter (dmin). The experimental animals were randomly divided into five groups (Group A, B, C, D, and E, with 6 in each group). Group A was the blank control group (normal saline), group B was the blank microsphere embolization group (6.5 mg of blank microspheres, Peking University School of Pharmacy), group C was the drug-loaded microsphere embolization group (2 mg of ADM, Pharmacia Upjohn, Italy + 6.5 mg of drug-loaded microspheres), group D was the lipiodol embolization group (0.8 ml of UFLP, Gabor, France), and group E was the ADM + lipiodol embolization group (2 mg of ADM + 0.8 ml of UFLP). This study was carried out in strict accordance with the recommendations in the Guide for the Care and Use of Laboratory Animals of the National Institutes of Health. The animal use protocol has been reviewed and approved by the Institutional Animal Care and Use Committee (IACUC) of Shenzhen Hospital of Southern Medical University.

#### Observation indexes and methods

All the animals were performed liver and lung thin-layer CT examination (PHILIPS Intergis Allura angiography machine) 3 weeks after embolization or chemoembolization to observe the liver and the conditions of intra-tumor iodized oil deposition and tumor necrosis. The animals were then killed and observed the liver specimens and abdominal organs, including the largest diameter (dmax) and the smallest diameter (dmin) of the tumor and the necrotic area. Partial tumor, peritumoral, and liver specimens were fixed in 4% paraformaldehyde, and

the tumor volume, growth rate, and tumor necrotic rate were calculated according to the following formula: tumor volume (V) = 1/2 dmax × dmin<sup>2</sup>. Tumor growth rate = volume at the end Week 5 (V5) - volume at the end Week 2 (V2)/V2 × 100%. Tumor area = (π/4) maximum diameter of the section (dmax) × vertical length of the maximum diameter (b). Tumor necrotic rate = necrotic area (cm<sup>2</sup>)/tumor area (cm<sup>2</sup>) × 100%. At the same time, the sampled liver specimens were fixed and cut with a layer thickness of 5 mm, and 6 sections were randomly selected for H&E staining and microscopy. According to the CT images (GE Lightspeed 16-slice spiral CT machine) and gross anatomy, the distant metastasis of the lung, peritoneal cavity, and adjacent organs was carefully observed.

At the same time, conventional paraffin-embedded sections were prepared and determined the VEGF-positive cells (Boster German) by semi-quantitative method. The standards of judging positive staining cells were: <5%: negative (-); 5-15%: weakly positive (+); 16-50%: positive (++); >50%: strongly positive (+++) [8]. The counting method of microvessels referred to the method of Kim et al. [14] (Beijing Zhongshan Company); the TUNEL method (TdT-mediated dURP nick and Labeling) was performed to detect the apoptosis (Boster German).

#### Statistical analysis

The data were analyzed and processed using SPSS11.0 statistical software. The measurement data were expressed by mean ± standard deviation. The comparison of measurement data among groups used the analysis of variance. The SNK-q test was used for the comparison between two groups. The comparison of count data was performed by the Pearson Chi-square test and Fisher's exact probability Chi-square test. The semi-quantitative grade data were analyzed using the Spearman rank correlation analysis.

### Results

#### Observation of growth and metastasis of rabbit liver VX2 xenografts

In this study, the liver implanted tumors in all the 30 rabbits swelled or showed invasive growth. The enhanced CT 2 weeks before surgery

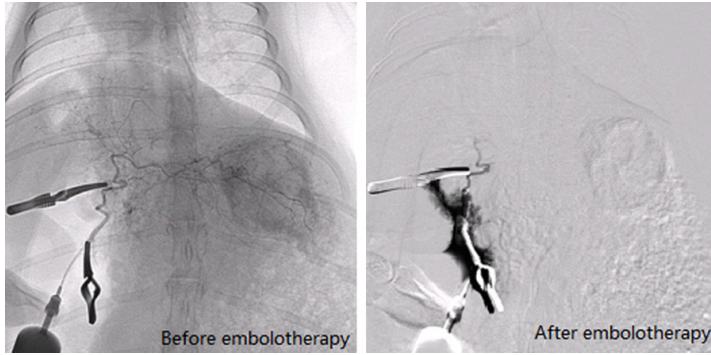


**Figure 1.** Blood supply before and after embolotherapy of VX2 transplanted tumor.

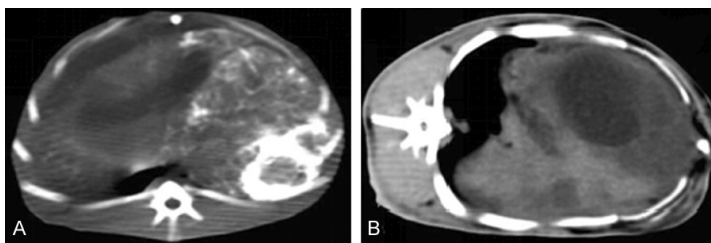


**Figure 2.** Thin-layer CT after embolization: iodized oil selectively deposited in the tumor area.

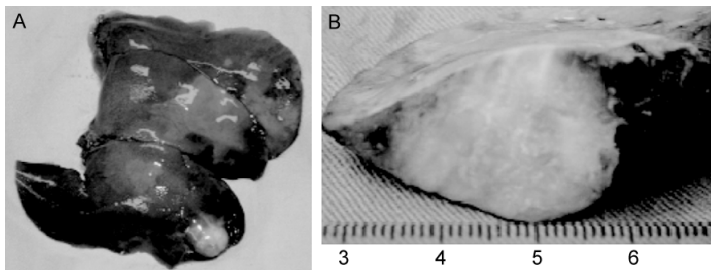


**Figure 3.** Tumor tissue of gross specimen. A: Before embolotherapy (group A). B: After embolotherapy (group C).

**Table 1.** Growth and necrotic rates and TUNEL test results of liver VX2 xenografts

Group	HE staining		TUNEL detection Positive rate (%)
	Growth rate (%)	Necrotic rate (%)	
A	6812.46±2409.48	16.16±0.27	0.3±0.12
B	206.36±4.57 <sup>a</sup>	53.45±1.47 <sup>a</sup>	11.4±2.16 <sup>a</sup>
C	115.45±14.07 <sup>a,b</sup>	56.58±1.62 <sup>a,b</sup>	14.3±3.65 <sup>a,b</sup>
D	5648.15±413.09 <sup>a,c</sup>	29.73±0.51 <sup>a,b,c</sup>	1.7±0.27 <sup>a,b,c</sup>
E	787.64±57.92 <sup>a,b,c,d</sup>	36.54±5.44 <sup>a,b,c</sup>	5.1±1.38 <sup>a,b,c,d</sup>

Note: Compare with group A, <sup>a</sup>P<0.05; compare with group B, <sup>b</sup>P<0.05; compare with group C, <sup>c</sup>P<0.05; compare with group D, <sup>d</sup>P<0.05.

showed that the tumor was round or elliptical, with peripheral enhancement, uneven central enhancement, and occasional liquefaction

necrosis. In hepatic angiography, the rabbit VX2 transplanted tumor had rich blood supply (**Figure 1**) and showed obvious early tumor angiography and parenchymal staining, especially in the peripheral part of the tumor. Thin-layer CT after embolization showed that iodized oil selectively deposited in the tumor area, particularly dense in the peripheral part, and large liquefaction necrosis was observed in the central part (**Figure 2**). The tumor tissue of gross specimen showed cheese-like changes (**Figure 3**). Intra-tumoral hemorrhage, cholestasis, and bile leakage were also observed in the liver specimens during embolization treatment (**Figure 3**).

*Effects of different treatments on growth of rabbit liver VX2 orthotopic liver xenografts*

The tumor growth rate and necrotic rate of the xenografts in each group are shown in **Table 1**. Intrahepatic and distant metastasis occurred in group A and group D, followed by 66.7% of intrahepatic and distant metastasis in group E, 50% of intrahepatic metastasis and 33.3% of distant metastasis in group B, and 33.3% of intrahepatic metastasis and 16.7% of distant metastasis in group C.

Angiography in Week 2 of the experiments showed tumor staining, but after the sodium alginate microspheres or ADM-alginate microspheres were injected via the hepatic artery, the blood supply to the tumor was interrupted. There was no significant difference in the volume of tumor between group A and other groups at the end of Week 5. The tumor volume in each group increased after treatment. The tumor volumes in group A and group D were 64.49 ± 2.54 mm and 68.62 ± 19.60 mm, respectively, but the tumor volumes in group E (9.83 ± 5.10 mm), group B (3.60 ± 1.07 mm), and group C (2.22 ± 0.71 mm) significantly reduced

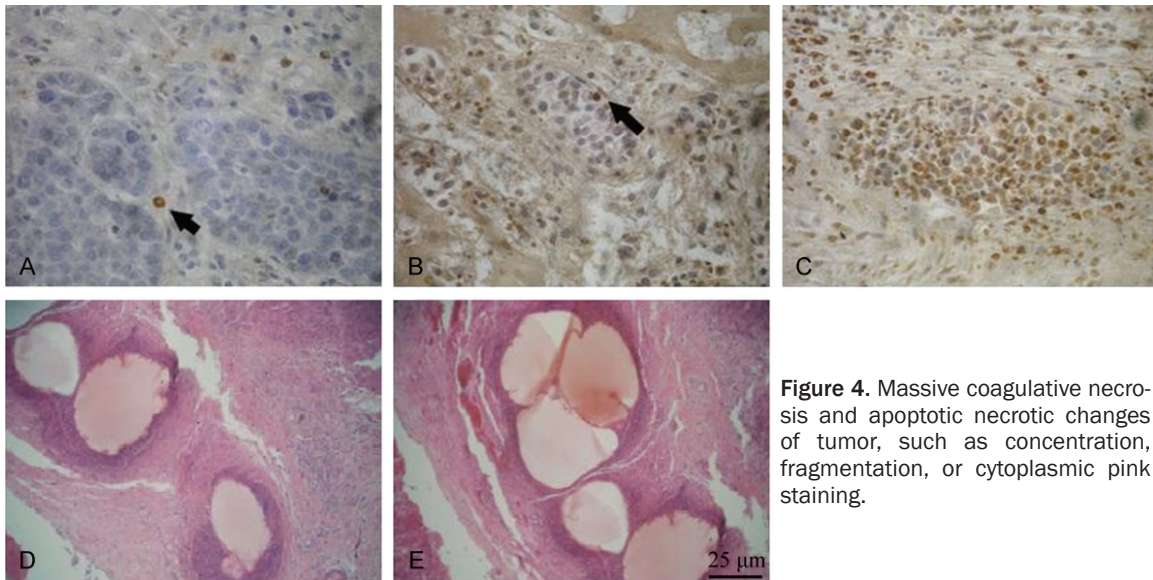


**Figure 4.** Massive coagulative necrosis and apoptotic necrotic changes of tumor, such as concentration, fragmentation, or cytoplasmic pink staining.

**Table 2.** VEGF staining and MVD counts in different groups

Group	n	VEGF positive			Positive rate (%)	MVD count
		+	++	+++		
A	6	1	1	2	66.7	55.36±7.02
B	6	1	0	2	50	41.27±8.45 <sup>a</sup>
C	6	3	1	2	100	82.42±6.23 <sup>a,b</sup>
D	6	1	3	1	83.3	67.81±11.42 <sup>b,c</sup>

Note: Compared with group A, <sup>a</sup>P<0.05; compare with group B, <sup>b</sup>P<0.05; compare with group C, <sup>c</sup>P<0.05. Spearman rank correlation analysis between VEGF and MVD shows a correlation coefficient of 0.726, P<0.01.

(P<0.05). Peritoneal metastasis was mainly characterized by peritoneal thickening in enhanced CT, as well as massive ascites in the perihepatic and abdominal cavity (**Figure 3**). After embolization, the tumor cells in the central part of the tumor showed massive coagulative necrosis, and a large number of tumor cells were found apoptotic necrotic changes such as concentration, fragmentation, or cytoplasmic pink staining in the part close to the periphery (**Figure 4**).

#### VEGF immunohistochemistry results and MVD count

Immunohistochemistry results: normal liver tissue and peritumoral liver tissue have no staining or only very weak staining. The positive rates of VEGF expression in group A, B, C, and D were 66.7%, 50%, 100%, and 83.3%, respectively. There was no significant difference in the comparison among the four groups (P>0.05).

CD31 staining and MVD count: the endothelial cells showed different degrees of brown-yellow to brown staining in the tumor tissue. In this experiment, the MVD counts were 55.36 ± 7.02, 41.27 ± 8.45, 82.42 ± 6.23, and 67.81 ± 11.42, respectively (**Table 1**). The MVD value in group D was higher than group B and group C, and the MVD value in group D was lower than group E (P<0.05). The Spearman rank correlation analysis between VEGF and MVD showed a correlation coefficient of 0.726, P<0.01 (**Table 2**).

Three weeks after TACE, the gross specimen showed liquefaction necrosis in the central part of the tumor, but residual tumor parenchyma still remained certain white fish-like tissue in the periphery of the tumor. In the specimens with positive TUNEL staining, more nuclear enlargement, cytoplasm with deeply-stained brown granules, and fragmentation and concentration of nucleoli can be observed at the junction of irregular necrotic center/surrounding area of the tumor with the boundary of residual tissue, suggesting apoptosis of a large number of tumor cells (**Figure 5**). The apoptotic indexes in the five groups were: 0.3%, 11.4%, 14.3%, 1.7%, and 5.1%, respectively (P<0.01). There were scattered apoptotic cells in group A, and apoptotic cells in each embolization group increased, mainly locating in the periphery of the tumor, and the apoptotic cells in group B also increased significantly. The comparison among groups B-D showed that the apoptotic cells in group C and D significantly increased. In the normal liver tissue of group E, a large num-

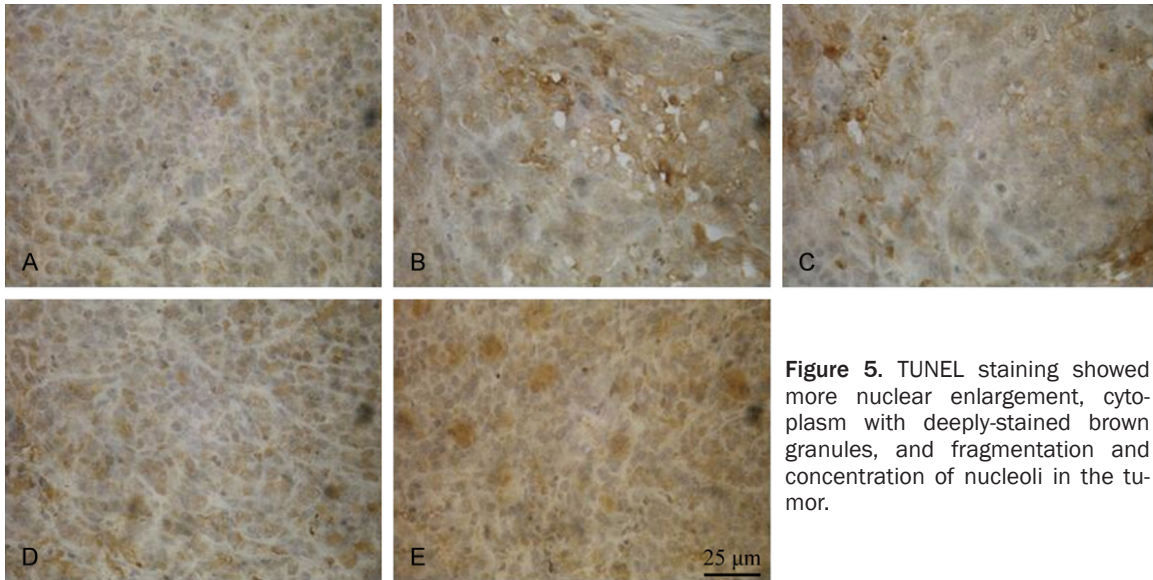


**Figure 5.** TUNEL staining showed more nuclear enlargement, cytoplasm with deeply-stained brown granules, and fragmentation and concentration of nucleoli in the tumor.

ber of apoptotic normal hepatocytes with positive TUNEL staining were found.

### Discussion

#### *Anti-tumor mechanism of sodium alginate*

There is now more and more evidence indicating that [15, 16], in addition to causing embolization by itself, TACE may cause recurrence of residual foci, and different embolic agents also affect the long-term efficacy of TACE. The traditional embolic agent lipiodol has a short residence time in tumor blood vessels, and because of its liquid state, it is difficult to achieve complete embolization due to siphon action and blood flow in tumor blood vessels [17], so chemotherapy drugs can achieve effective distribution. In this study, ADM-alginate microspheres were used as the embolic agent. Due to their good and rapid expansion characteristics, after the microspheres reached the target blood vessels, the volume can rapidly expand to twice as much as the original, so the tumor blood supply artery can be rapidly occluded. The effects of tumor necrosis were more complete than iodized oil embolization. The rapid necrosis of the tumor preceded the establishment of residual blood supply, which greatly reduced the recurrence of residual tumor. At the end of Week 5, the growth of liver VX2 xenografts in group C was more inhibited than group B and group D, and the tumor necrotic rate was greater. Although simple lipiodol embolization and conventional chemoembolization had a certain inhibitory effect on the

growth of orthotopic transplantation tumors, their inhibitory effects against intrahepatic metastasis and distant metastasis were not significant when compared with group A. The application of ADM in TACE can not only further inhibit the growth of orthotopic liver xenografts but also significantly lower the intrahepatic metastasis rate and distant metastasis rate than group A, B, and D.

#### *Role of angiogenic factors such as VEGF in tumor angiogenesis*

Tumor angiogenesis is particularly important in tumor recurrence and metastasis. Due to the incomplete vascular structure of the tumor, the intercellular connections are relaxed, so the tumor cells can directly enter the blood without invasion. During invasion, the tumor cells can release various factors and proteolytic enzymes to promote the metastasis of liver tumor cells. In patients with liver cancer, the VEGF concentration is statistically high in patients with tumor diameter >5 cm, tumor thrombus, or microscopic tumor thrombus ( $P < 0.05$ ). Tumor angiogenesis is essential for tumor growth and metastasis. Studies have reported that basic fibroblast growth factor (bFGF) is the strongest vascular endothelial growth factor, followed by the vascular endothelial growth factor (VEGF) and the platelet-derived endothelial cell growth factor (PD-ECGF) [18]. VEGF is a well-known cytokine that promotes the vascular endothelial growth and has the functions of increasing the microvascular permeability, promoting the

endothelial cell division and vascular construction from different sources, promoting the endothelial cell migration, and the inducing tumor angiogenesis. It is closely related to the growth of solid tumors and the metastasis of malignant tumors [19, 20].

### *Tumor angiogenesis after embolization.*

In this study, expression of VEGF and MVD in group D was significantly higher than group B ( $P < 0.05$ ), but the expression showed a decrease in group C compared with group B, indicating that VEGF expression increase and angiogenesis are in the process of tumor growth. The expression of VEGF increased significantly after embolization with simple lipiodol, and the angiogenesis of tumor was more obvious. The application of ADM in the process of ADM microsphere embolization reduced expression of VEGF in tumors and inhibited the tumor angiogenesis to a certain extent. Moreover, rapid and effective expansion of the sodium alginate microspheres made the embolization more thorough, reduced retention of residual foci, and inhibited tumor recurrence for a period of time.

### *Evaluation of ADM-alginate microsphere embolization*

This study found that ADM-alginate microspheres can significantly inhibit the tumor volume growth than simple sodium alginate microspheres, resulting in a larger necrotic area ( $P > 0.05$ ), significantly reduced microvascular angiogenesis ( $P < 0.05$ ), and significantly reduced distant metastasis ( $P < 0.05$ ). Therefore, ADM-alginate microspheres can significantly improve the effect of TACE treatment, especially in inhibiting tumor distant metastasis.

Kerr et al. [21] first proposed the concept of apoptosis in 1972, which described the apoptosis from a morphological point of view, and considered it to be a basic biological phenomenon that maintains the balance of tissue dynamics. At present, TACE is the main non-surgical method against primary liver cancer because TACE can not only promote necrosis of HCC but also effectively promote the apoptosis, thus playing a role of inducing the apoptosis of tumor cells by affecting apoptosis-related genes with embolism-related effects [22].

Sodium alginate microspheres have good biocompatibility, and the final degradation products in the body are non-toxic polysaccharides, mannose, and gulose, which are mainly excreted by the kidneys. Therefore, the apoptosis-inducing effect of ADM-alginate microspheres is mainly related to the effects of the chemotherapeutic drugs embedded inside the embolic agents, such as damaging the DNA of tumor cells, increasing the expression of pro-apoptotic genes, inactivating the apoptosis-inhibiting genes, and causing ischemia and hypoxia in the tumor area.

### **Conclusion**

In conclusion, ADM-alginate microspheres have many advantages such as rapid blood supply cutoff and continuous induction of apoptosis of tumor cells, can significantly inhibit the growth and metastasis of orthotopic transplanted tumors. However, it should also be noted that at present, ADM-alginate microspheres are mainly characterized by strong antitumor effects in TACE. With deepening of research, sodium alginate microspheres containing different drugs may provide better pharmaceutical dosage forms and play important roles in anti-tumor growth and metastasis.

### **Disclosure of conflict of interest**

None.

**Address correspondence to:** Dandan Xiao, Department of Outpatient, Shenzhen Hospital, Southern Medical University, Shenzhen 518010, China. Tel: +86 10 2336 0604; Fax: +86 10 23323777; E-mail: cnkaiyuanxu@126.com

### **References**

- [1] Glantzounis GK, Tokidis E, Basourakos SP, Ntzani EE, Lianos GD and Pentheroudakis G. The role of portal vein embolization in the surgical management of primary hepatobiliary cancers. a systematic review. *Eur J Surg Oncol* 2017; 43: 32-41.
- [2] Petrowsky H and Busuttil RW. Resection or ablation of small hepatocellular carcinoma: what is the better treatment? *J Hepatol* 2008; 49: 502-504.
- [3] Shindoh J, Tzeng CW, Aloia TA, Curley SA, Huang SY, Mahvash A, Gupta S, Wallace MJ

## New embolic agent in liver transplantation tumors

- and Vauthey JN. Safety and efficacy of portal vein embolization before planned major or extended hepatectomy: an institutional experience of 358 patients. *J Gastrointest Surg* 2014; 18: 45-51.
- [4] Li D, Kang J and Madoff DC. Locally ablative therapies for primary and metastatic liver cancer. *Expert Rev Anticancer Ther* 2014; 14: 931-945.
- [5] Simon CJ, Dupuy DE and Mayo-Smith WW. Microwave ablation: principles and applications. *Radiographics* 2005; 25: S69-83.
- [6] Maruyama H, Yoshikawa M and Yokosuka O. Current role of ultrasound for the management of hepatocellular carcinoma. *World J Gastroenterol* 2008; 14: 1710-1719.
- [7] de Graaf W, van den Esschert JW, van Lienden KP, van Gulik TM. Induction of tumor growth after preoperative portal vein embolization: is it a real problem? *Ann Surg Oncol* 2009; 16: 423-430.
- [8] Chung JW. Transcatheter arterial chemoembolization of hepatocellular carcinoma. *Hepato-gastroenterology* 1998; 45: 1236-1241.
- [9] Katayama N, Sugimoto K, Okada T, Ueha T, Sakai Y, Akiyoshi H, Mie K, Ueshima E, Sofue K, Koide Y, Tani R, Gentsu T and Yamaguchi M. Intra-arterially infused carbon dioxide-saturated solution for sensitizing the anticancer effect of cisplatin in a rabbit VX2 liver tumor model. *Int J Oncol* 2017; 51: 695-701.
- [10] Tomozawa Y, Nitta N, Ohta S, Watanabe S, Sonoda A, Nitta-Seko A, Tsuchiya K and Murata K. Anti-tumor effects of sorafenib administered at different time points in combination with transarterial embolization in a rabbit VX2 liver tumor model. *Cardiovasc Intervent Radiol* 2017; 40: 1763-1768.
- [11] Kim GM, Kim MD, Kim do Y, Kim SH, Won JY, Park SI, Lee do Y, Shin W and Shin M. Transarterial chemoembolization using sorafenib in a rabbit VX2 liver tumor model: pharmacokinetics and antitumor effect. *J Vasc Interv Radiol* 2016; 27: 1086-1092.
- [12] Akinwande O, Kim D, Edwards J, Brown R, Phillips P, Scoggins C and Martin RC 2nd. Is radioembolization ((90)Y) better than doxorubicin drug eluting beads (DEBDOX) for hepatocellular carcinoma with portal vein thrombosis? a retrospective analysis. *Surg Oncol* 2015; 24: 270-275.
- [13] Chen J, Qian T, Zhang H, Wei C, Meng F and Yin H. Combining dynamic contrast enhanced magnetic resonance imaging and microvessel density to assess the angiogenesis after PEI in a rabbit VX2 liver tumor model. *Magn Reson Imaging* 2016; 34: 177-182.
- [14] Kim DY, Choi MS, Lee JH, Koh KC, Paik SW, Yoo BC, Shin SW, Choo SW, Do YS and Rhee JC. Milan criteria are useful predictors for favorable outcomes in hepatocellular carcinoma patients undergoing liver transplantation after transarterial chemoembolization. *World J Gastroenterol* 2006; 12: 6992-6997.
- [15] Poon RT, Ngan H, Lo CM, Liu CL, Fan ST and Wong J. Transarterial chemoembolization for inoperable hepatocellular carcinoma and postresection intrahepatic recurrence. *J Surg Oncol* 2000; 73: 109-114.
- [16] Trinchet JC, Ganne-Carrie N and Beaugrand M. Intra-arterial chemoembolization in patients with hepatocellular carcinoma. *Hepato-gastroenterology* 1998; 45: 1242-1247.
- [17] Iwai K, Maeda H and Konno T. Use of oily contrast medium for selective drug targeting to tumor: enhanced therapeutic effect and x-ray image. *Cancer Res* 1984; 44: 2115-2121.
- [18] Kumar R, Yoneda J, Bucana CD and Fidler IJ. Regulation of distinct steps of angiogenesis by different angiogenic molecules. *Int J Oncol* 1998; 12: 749-757.
- [19] Kobayashi N, Ishii M, Ueno Y, Kisara N, Chida N, Iwasaki T and Toyota T. Co-expression of bcl-2 protein and vascular endothelial growth factor in hepatocellular carcinomas treated by chemoembolization. *Liver* 1999; 19: 25-31.
- [20] An FQ, Matsuda M, Fujii H and Matsumoto Y. Expression of vascular endothelial growth factor in surgical specimens of hepatocellular carcinoma. *J Cancer Res Clin Oncol* 2000; 126: 153-160.
- [21] Kerr JF, Wyllie AH and Currie AR. Apoptosis: a basic biological phenomenon with wide ranging implication in tissue kinetics. *Br J Cancer* 1972; 26: 239-257.
- [22] Okada S. Transcatheter arterial embolization for advanced hepatocellular carcinoma: the controversy continues. *Hepatology* 1998; 27: 1743-1744.